Journal of Structural Geology, Vol. 6, No. 3, pp. 293 to 302, 1984
Printed in Great Britain

0191-8141/84 $03.00 + 0.00

Quartz microfabric of the Laxfordian Canisp Shear Zone, NW Scotland

LARS N. JENSEN

Department of Geology, Aarhus University, C. F. Møllers Alle, DK-8000 Aarhus C. Denmark

(*Received* 23 *April* 1982, *accepted in revised form* 4 *October* 1983)

Abstract—The Canisp Shear Zone transects layered Lewisian gneisses near Lochinver, NW Scotland. It is a vertical ductile shear zone with a dextral shear sense, formed during Laxfordian amphibolite facies metamorphism, transposing the layering to new foliation and linear structures. Minerals in the layered gneisses show little or no shape fabric, while a strong shape fabric defines the foliation. For quartz, this shape fabric is accompanied by development of a preferred crystal orientation with fabric patterns reflecting the geometry of the shear deformation. The quartz fabric shows a pole-free area around the lineation with the *c*-axes concentrated in an asymmetric cross-girdle or a point maximum perpendicular to the shear plane, and a monoclinic symmetry consistent with the shear sense.

INTRODUCTION

LEWISIAN gneisses on the Scottish mainland (Fig. 1) are affected by three major Precambrian metamorphic episodes of regional extent (Park 1970). A flat-lying, gently undulating layering (S_L) was formed in the mainly tonalitic complex during the Scourian granulite facies episode. The succeeding Inverian amphibolite facies episode is characterized by widespread retrogression, folding around NW–SE subhorizontal axes, and intrusion of doleritic and (later) ultrabasic dykes. In the central part of the Lewisian outcrop, deformation in narrow vertical zones during the Laxfordian amphibolite facies episode caused further retrogression and formation of a new foliation (S_{SH}) and linear structures (L_{SH}). These zones are now regarded as ductile shear zones (e.g. Ramsay & Graham 1970, Beach 1974).

The mapped area shows evidences of all three Lewisian episodes including the Inverian Lochinver antiform (Evans & Lambert 1974) and parts of the Laxfordian Canisp Shear Zone. Following a brief description of the structures and microstructures of the gneisses, this paper focuses on the development of preferred orientation of quartz in relation to the shear episode. The purpose is to show the symmetry relations between the fabric and the shear deformation, to infer the operative slip systems from the fabric patterns and to attempt to resolve the confusion concerning the shear sense of the Canisp Shear Zone.

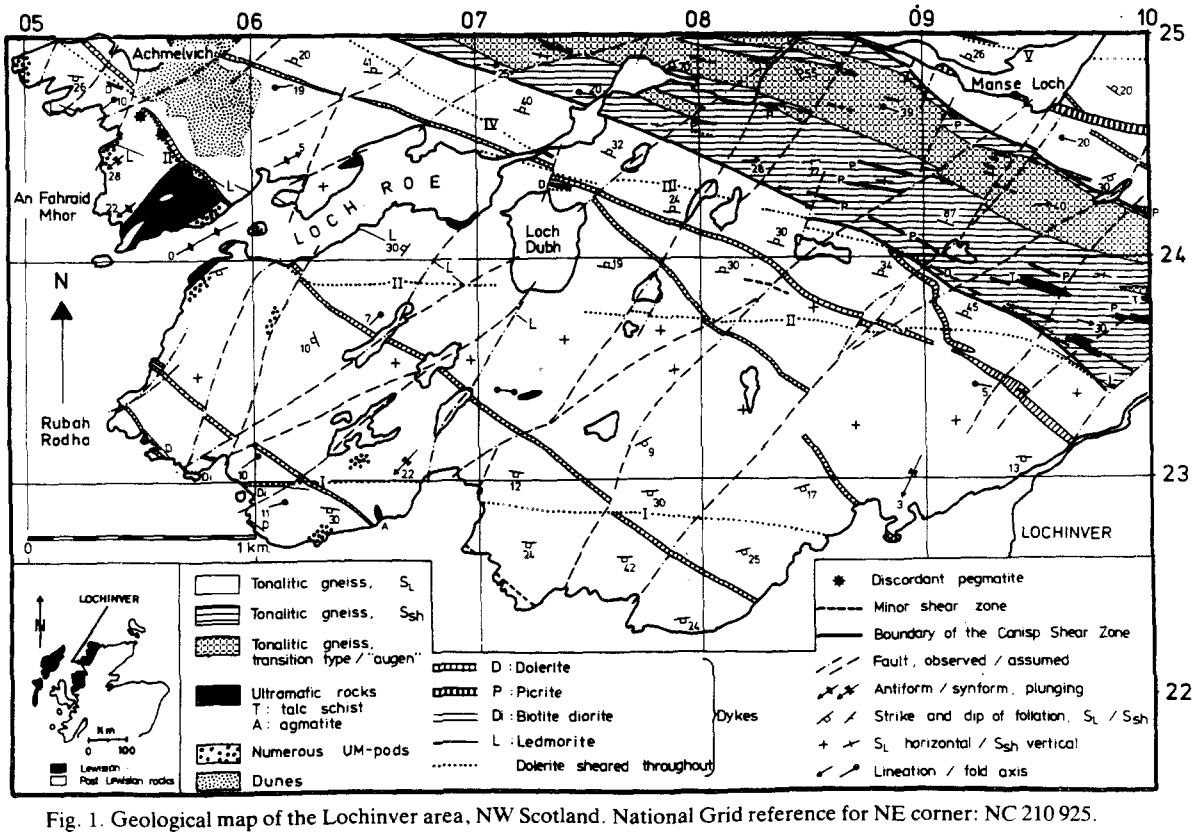

Fig. 1. Geological map of the Lochinver area, NW Scotland. National Grid reference for NE corner: NC 210 925.

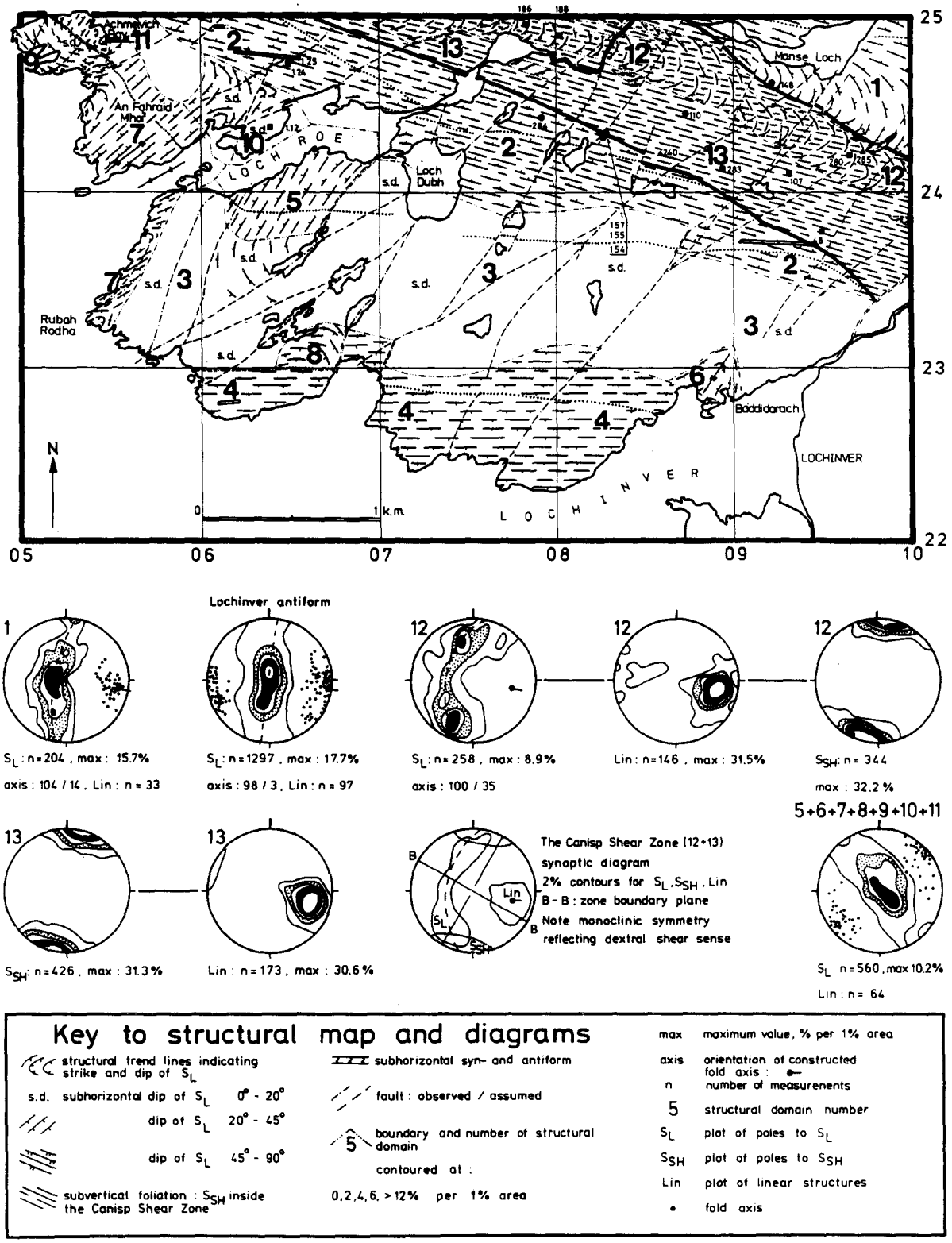

Fig. 2. Structural interpretation of the Lochinver area. Solid symbols with numbers indicate sample locations. Triangle: sample analysed for quartz shape fabric. Square: sample analysed for quartz *c*-axis fabric. Circle: sample analysed for quartz shape and *c*-axis fabric.

STRUCTURES AND MICROSTRUCTURES

Greyish, medium grained gneisses of tonalitic composition cover about 90% of the map area (Fig. 1). These gneisses are a heterogeneous mixture of acidic, intermediate (most common) and mafic types and it was not possible to establish marker horizons for structural analysis (cf. Sheraton *et al.* 1973). Based on the nature of the mesoscopic planar structures the gneisses are divided into three groups:

Group I. Layered gneisses are dominant outside the Canisp Shear Zone. The foliation (S_L) is defined by 0.5–5 cm thick layers of contrasting mineral assemblages, light layers are rich in plagioclase and quartz and dark layers are rich in hornblende and biotite (Fig. 3a). S_L is normally most pronounced in gneisses of

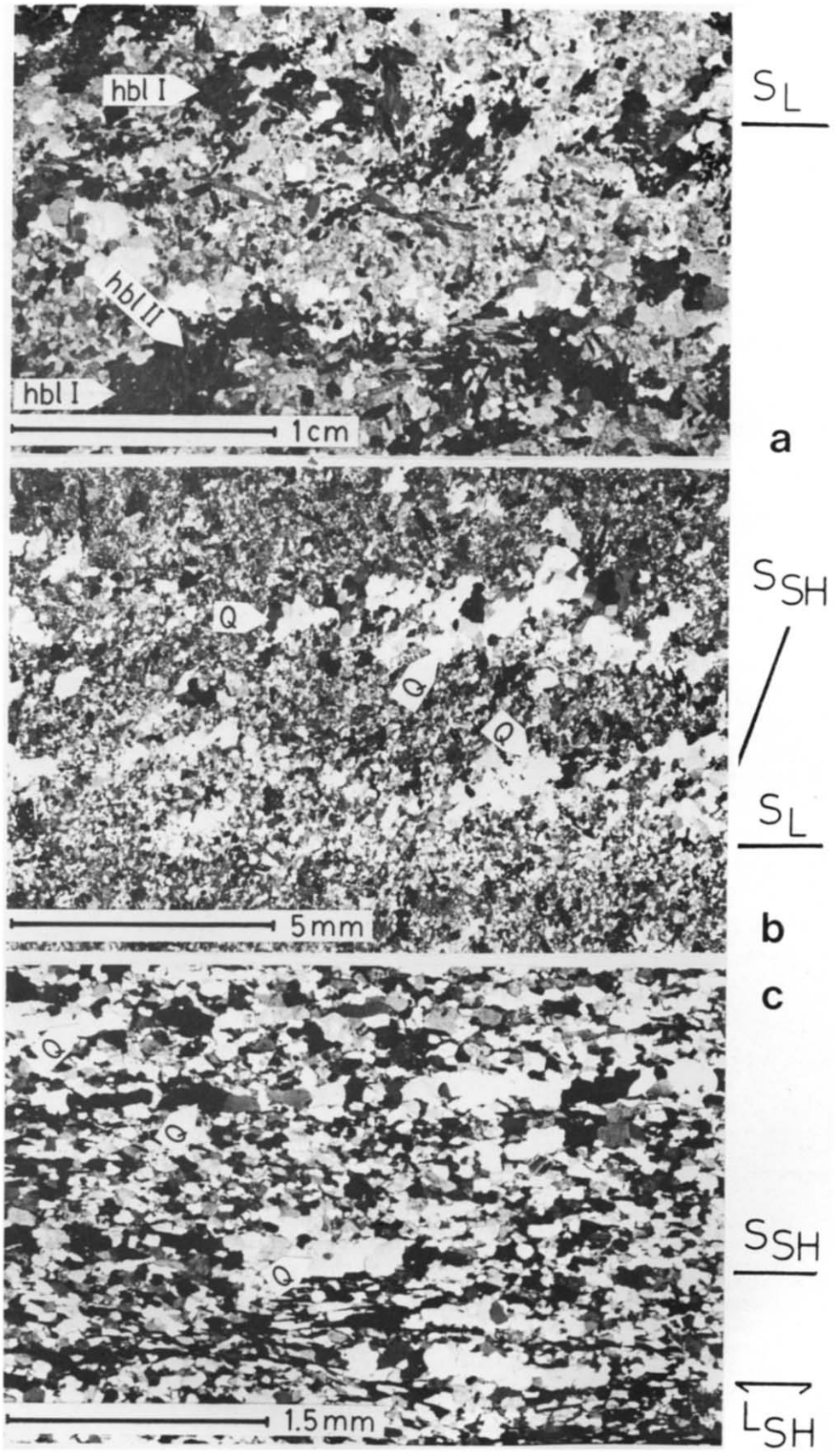

Fig. 3. Typical microstructures of the three gneiss types. (a) Layered gneiss without grain shape fabric. Hornblende labelled I are relict grains and those labelled II are clusters of recrystallized grains. (b) Gneiss where both layering (S_L) and schistosity (S_{SH}) are visible. Quartz aggregates (Q) have a shape fabric parallel to S_L while their constituent grains show a weak shape fabric parallel to S_{SH}. (c) Schistose gneiss with a good grain-shape fabric and a strong shape fabric of the quartz aggregates (Q).

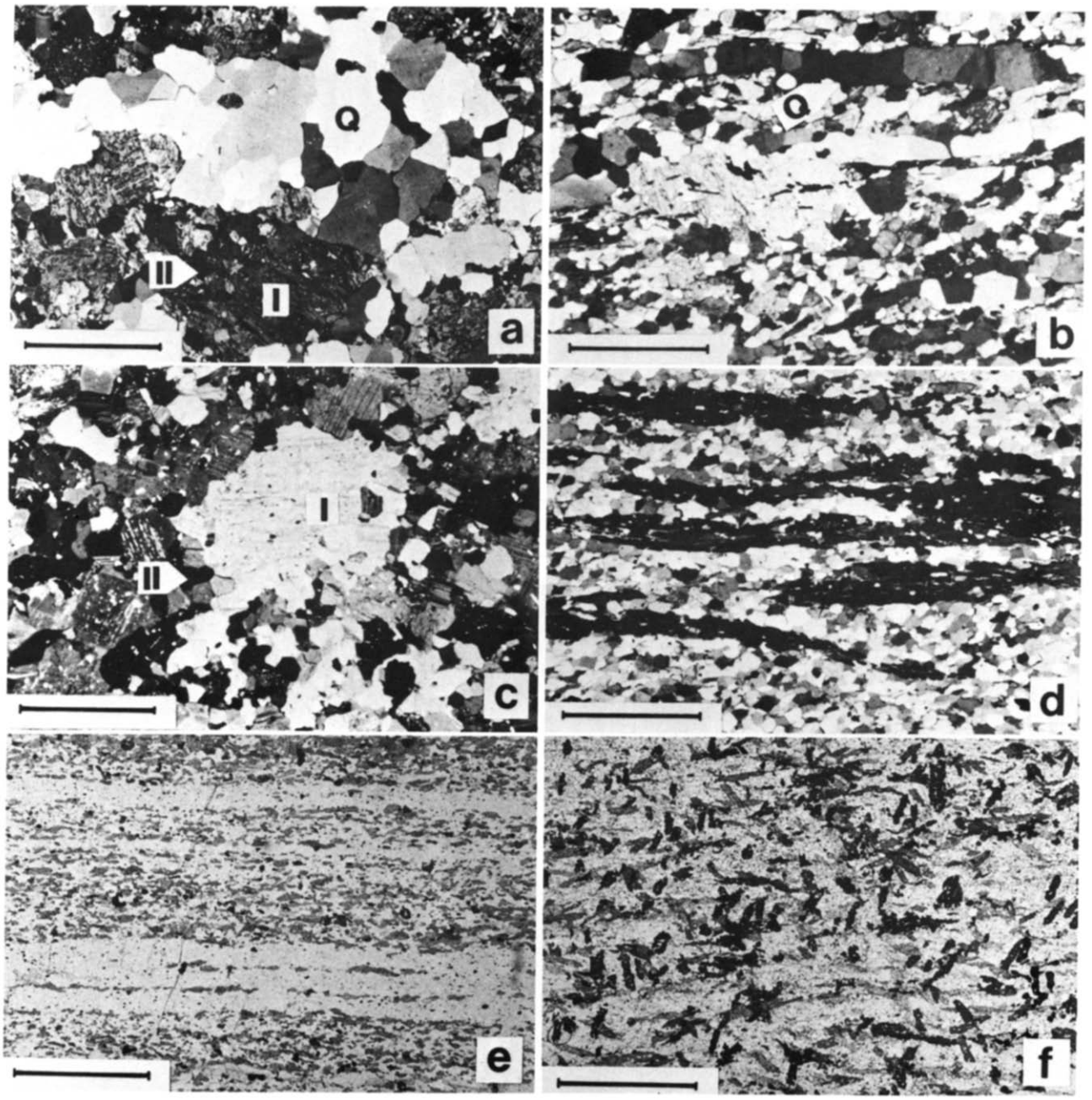

Fig. 4. Typical microstructures of quartz, plagioclase and hornblende in layered and schistose gneisses. (a) Layered gneiss with quartz aggregates of polygonal grains (Q) surrounded by relict (I) and recrystallized (II) plagioclase grains. S_L is E–W and the scale bar is 1.2 mm long. (b) Schistose gneiss cut perpendicular to S_{SH} and parallel to L_{SH}. Ribbon-like quartz aggregates (Q) of elongated polygonal grains with (prismatic) subgrain-walls perpendicular to S_{SH}, surrounded by plagioclase with a polygonal texture. The scale bar is 1 mm long. (c) Layered gneiss with a heterogeneous polygonal texture of relict (I) and recrystallized (II) plagioclase grains. Dusty appearance of plagioclase is due to clouding and numerous inclusions of epidote and white mica. The scale bar is 1 mm long. (d) Schistose gneiss (cut perpendicular to S_{SH} and parallel to L_{SH}) with a polygonal texture of plagioclase and a mineral lineation of hornblende formed by syn-tectonic growth (note subgrains, bent crystals and inclusions). The scale bar is 1 mm long. (e) Schistose gneiss cut perpendicular to S_{SH} and L_{SH}. Plane polarized light. Grain shape and pleochroism shows the very strong preferred orientation of hornblende, darker grains are those deviating from the preferred orientation. The scale bar is 1 mm long. (f) Schistose gneiss (cut perpendicular to S_{SH} and parallel to L_{SH}. Plane polarized light) showing a graben structure formed by post-tectonic growth of hornblende. The scale bar is 1 mm long.

intermediate composition, but single layers can seldom be followed for more than a few metres. The constituent mineral grains show little or no shape fabric while mineral aggregates of quartz, hornblende or biotite may show a good shape fabric parallel to S_L.

Group II. A transitional type (Fig. 1) where both S_L and S_{SH} are visible (Fig. 3b) occurs at the margin and in the less deformed central part of the Canisp Shear Zone (Fig. 2, domain 12).

Group III. Gneisses with a schistosity (S_{SH}) and with or without an incipient layering occur only in the most deformed part of the Canisp Shear Zone (Fig. 2, domain 13) and contemporaneous minor shear zones (Fig. 1). A pronounced shape fabric of the constituent mineral grains and mineral aggregates characterize the sheared gneisses (Fig. 3c), in particular the strong parallelism of biotite and/or hornblende defines S_{SH}. Hornblende crystals form a penetrative mineral lineation when parallel (Figs. 4d & e), and a garben structure (as defined by Spry 1969) when randomly oriented (Fig. 4f).

A synthesis of the structural analysis is presented in Fig. 2. The macroscopic structural domains are homogeneous with respect to at least one of the penetrative mesoscopic structural elements (S_L, S_{SH}, L_{SH}), and comprise a fold (e.g. domain 1), several parallel folds (e.g. domain 7) or part of a major fold as the Lochinver antiform (=domains 2–4).

Upright open folds with NE–SW axial trends dominate in domains 5–11. S_L is folded on mesoscopic and macroscopic scales, and the ultramafic body at An Fahraid Mhor (Fig. 1) is incorporated in these folds.

Three major antiforms (without intervening synforms) with WNW–ESE axial trends underlie the central and eastern part of the map area. Domain 1 is an open, upright, plunging antiform, while domains 2, 3 and 4 comprise the upright, open, subhorizontal Lochinver antiform (Fig. 2). The fold in domain 12 is close, upright and plunging, it is regarded as a WNW–ESE fold modified by later shearing. The doleritic dykes intruded prior to the ultrabasic dykes, and both types cut all the structures mentioned above.

Domain 13 is the most deformed part of the heterogeneous Canisp Shear Zone (=domain 12 and 13). S_{SH} is vertical and L_{SH} consists of a penetrative mineral lineation parallel to the axes of upright, close to isoclinal mesoscopic folds which plunge ESE (Fig. 2). The Canisp Shear Zone is discontinuous, as defined by Burg & Laurent (1978), S_L is transposed to S_{SH} within transition zones normally less than 5 m wide. The shear zone boundary planes are vertical with a strike of 120°, the shear direction is parallel to the projection of L_{SH} (the orientation of L_{SH} maximum in domain 13 = 105/30) into the boundary planes, giving 120/30, and the shear sense is dextral (note monoclinic symmetry of synoptic diagram, Fig. 2). Taking S_{SH} as the XY plane and L_{SH} as the X direction of the finite strain ellipsoid ($X \geq Y \geq Z$), shear strains of $\gamma = 3.5$ for domain 13 and $\gamma = 2.4$ for domain 12 are calculated using eq. (36) of Ramsay & Graham (1970).

Microstructures

To show how the shear episode changed the microstructures in the gneisses, microstructures in the major minerals of the layered gneisses are described and compared to microstructures of these minerals in the sheared gneisses (Fig. 4). Average modal content, modal range and grain size for each mineral are given in brackets.

Quartz (20.7%, 1.1–35.4%). In the layered gneisses quartz occurs mainly as aggregates in the approximate shape of oblate spheroids with the short axis at right angles to S_L (Fig. 5). The aggregates show an equilibrium microstructure of equant to elongated grains (0.05–1 mm) with an average diameter of 0.18 mm, weak undulatory extinction is common and a few grains show banded extinction with prismatic subgrain-walls (Fig. 4a). The shape and internal features of isolated grains are identical with those in the aggregates, but the grain size is slightly smaller (0.02–0.3 mm).

In the sheared gneisses, quartz occurs as isolated grains and as strongly elongated (ribbon-like) aggregates parallel to S_{SH} and L_{SH} (Figs. 4b, and 5). The grains are

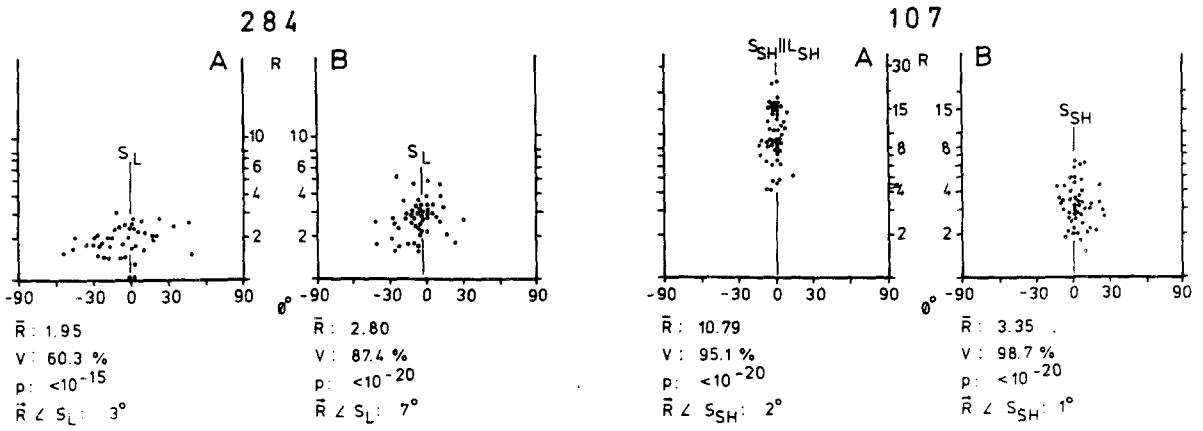

Fig. 5. R/Ø diagrams showing shape fabric of quartz aggregates. Sample 284 is a layered gneiss and sample 107 is a L-S tectonite from the Canisp Shear Zone. Average axial ratio for sample 284 is 1.03 : 1 : 0.45 giving a k-value (Flinn 1962) of 0.03, while mean axial ratio for sample 107 is 2.93 : 1 : 0.30 giving k 0.88. $\mathbf{R} \angle S_L$ or S_{SH} indicate the angle between resultant vector **R** and mesoscopic structure. See text for explanations of $\bar{R}$, V% and p.

elongate, and have a marked shape fabric, the common prismatic subgrain-walls are perpendicular to S_{SH} (Fig. 4b). The grain size of quartz varies from 0.02 to 0.3 mm and the average grain size in the Canisp Shear Zone is 0.07 mm.

Plagioclase (50.8%, 20.3–68.7%, An 25–32). In the layered gneisses plagioclase has a mortar to heterogeneous polygonal microstructure (Brown *et al.* 1980, figs. 2b & c) of relict grains (0.5–5 mm, plag I) surrounded by an equilibrium mosaic of (0.02–0.3 mm) recrystallized grains (plag II, Fig. 4c). In the shear zone only plag II (0.02–0.06 mm), with a polygonal microstructure and a weak shape fabric, is found (Fig. 4d). This complete recrystallization of relict grains provides the main contribution to the overall reduction in grain size of the gneisses, from 0.29 mm in the layered gneisses to 0.07 mm in the shear zone. These grain sizes have been determined by the method of Etheridge & Wilkie (1979) and 1200 grains were measured in each case.

Outside the Canisp Shear Zone hornblende (22.1%, 0–67.7%) occurs as relict grains 0.5–6 mm in diameter (hbl I) and as recrystallized grains 0.01–0.4 mm in diameter (hbl II, Fig. 3a). Within the shear zone there is further recrystallization of hbl I to hbl II with the development of a strong shape fabric (Fig. 4e). The mineral lineation is formed by syn-tectonic grain growth (Fig. 4d), and a graben structure by post-tectonic growth (Fig. 4f).

QUARTZ MICROFABRIC

Shape fabric

Relations between the mesoscopic structures and shape fabric of quartz grains have been analysed in ten samples (locations are shown in Fig. 2). Samples 154, 155, 157 and 1 are from a 100 m long traverse across the southern shear zone boundary, 154 and 155 are layered gneisses while 157 and 1 are from the 3 m wide transition zone.

The grain shape is approximated by an ellipse, and for each grain, the long axis (a), short axis (b) and the orientation of the long axis in relation to the trace of the foliation, ϕ, were measured. Two mutually perpendicular faces (A and B) were cut perpendicular to the

Table 1. Microstructural data.

	sample No.	orientation	modal % qz	d μ	$\bar{R}$	V %	random	p	angle between $\bar{R}$ and: S_L	S_{SH}	L_{SH}	n U/S	max	E.S.%	M0%	SD0%	M0% - 36.8% / SD0%
GROUP I	1.12	$\perp S_L$	17.8									200 U	5	42.33	42.23	3.28	1.66
	1.24	$\perp S_L$	6.4									200 U	6	39.67	42.86	3.54	1.71
	1.25	$\perp S_L$	4.9									200 U	7	40.49	39.20	3.12	0.71
	148A	$\perp S_L$	17.6	159	1.81	24.2	no	$<10^{-4}$	17°			200 U	7	38.85	37.28	4.11	0.12
	148B	$\perp S_L$		141	1.83	26.9	no	$<10^{-5}$	31°								
	154A	$\perp S_L$	12.2	164	1.83	18.8	no	<0.01	47°			200 U	7	42.54	43.58	1.81	3.69
	154B	$\perp S_L$		178	1.80	12.9	yes	>0.05	6°			200 U	6	40.29	41.19	3.93	1.12
	154 comb.											400 U	9	40.29	40.90	1.59	3.21
	155	$\perp S_L$	22.7									200 U	5	37.83	40.04	1.81	1.80
	284A	$\perp S_L$	29.8	209	1.74	8.1	yes	>0.3	50°			200 U	7	40.39	41.74	1.32	3.75
	284B	$\perp S_L$		137	2.03	33.2	no	$<10^{-5}$	18°								
GROUP II	1A	$\perp S_L \wedge S_{SH}$	35.4	203	1.86	23.5	no	$<10^{-4}$	25°	20°		200 U	8	40.08	40.06	1.39	2.35
	1B	$\parallel L_{SH} \wedge \perp S_L$		232	1.79	43.9	no	$<10^{-15}$			0°						
	157A	$\perp S_L \wedge S_{SH}$	17.3	154	1.85	26.1	no	$<10^{-5}$	75°	3°		200 U	6	42.74	41.29	3.15	1.43
	157B	$\parallel L_{SH} \perp S_{SH}$		152	1.82	54.7	no	$<10^{-20}$		2°	2°	200 U	6	43.15	41.15	2.13	2.23
	186A	$\perp S_L \wedge S_{SH}$	22.2	120	1.99	62.4	no	$<10^{-20}$	65°	7°		200 U	9	41.31	42.99	1.81	3.43
	186B	$\parallel L_{SH} \perp S_{SH}$		170	1.87	60.1	no	$<10^{-20}$		1°	1°	200 U	7	43.15	45.81	2.14	4.21
	188B	$\parallel L_{SH} \perp S_{SH}$	17.7									100 U	5	41.10	39.55	2.21	1.21
	280A	$\perp L_{SH} \wedge S_{SH}$	43.3									200 U	6	45.81	48.55	2.99	3.93
	285A	$\parallel L_{SH} \perp S_{SH}$	26.2	170	2.16	53.8	no	$<10^{-20}$		5°	5°						
	285B	$\perp S_L \wedge S_{SH}$		167	1.98	58.3	no	$<10^{-20}$	89°	1°							
GROUP III	3A	$\perp S_{SH} \wedge L_{SH}$	24.7	71	1.81	52.4	no	$<10^{-20}$		6°		300 U	6	41.92	41.51	2.07	2.28
	3B	$\parallel L_{SH} \wedge \perp S_{SH}$		79	2.32	84.7	no	$<10^{-20}$		4°	4°	50 S	10	63.80	60.31	3.08	7.64
	48	$\perp S_{SH} \wedge L_{SH}$	18.6									400 U	5	38.85	40.72	1.24	3.17
	107	$\parallel L_{SH} \wedge \perp S_{SH}$	29.4									100 S	12	60.74	59.56	2.94	7.74
	110A	$\perp S_{SH} \wedge L_{SH}$	23.4	86	2.49	85.9	no	$<10^{-20}$		0°		200 U	6	44.79	42.47	2.12	2.68
	110B	$\parallel L_{SH} \wedge \perp S_{SH}$		110	2.78	92.6	no	$<10^{-20}$		2°	2°	100 S	12	61.35	60.00	2.70	8.60
	240A	$\perp S_{SH} \wedge L_{SH}$	15.0	68	1.99	75.4	no	$<10^{-20}$		0°							
	240B	$\parallel L_{SH} \wedge \perp S_{SH}$		61	2.26	88.9	no	$<10^{-20}$		3°	3°						
	283	$\parallel L_{SH} \wedge \perp S_{SH}$	44.1									100 S	9	54.81	54.36	5.71	3.08

See text for further explanations

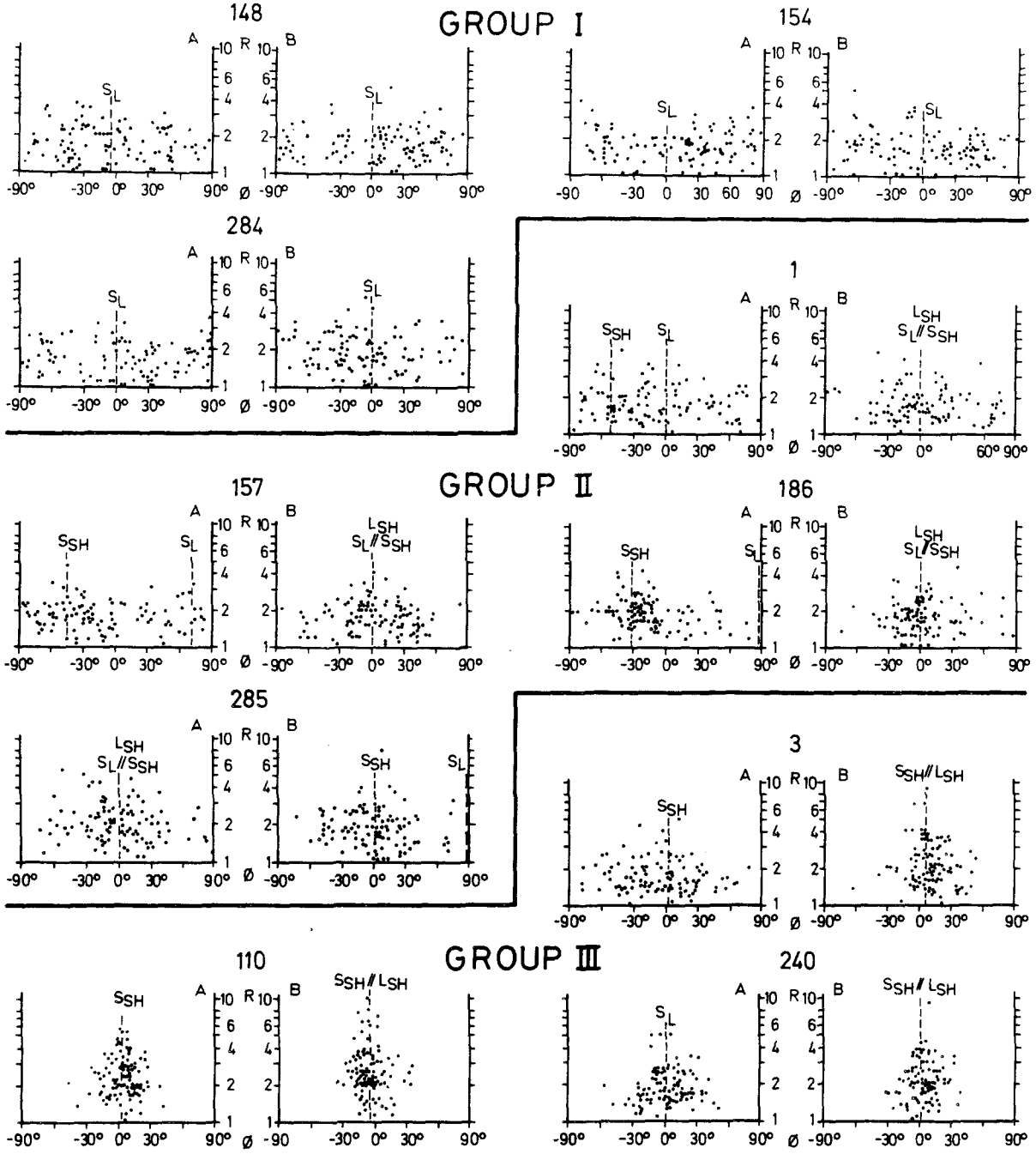

Fig. 6. *R*/Ø plots of shape fabric of quartz grains in gneisses from the three structural groups.

foliation in each sample. In the lineated samples one face is parallel and the other is perpendicular to the lineation. Table 1 gives the orientations of faces A and B in relation to S_L, S_{SH} and L_{SH} for each sample. The measurements of 100 grains in each face provide the basis for calculation of the following parameters: (1) the axial ratio of each grain (R) and the arithmetic mean of R ($\bar{R}$, Table 1) for each face. These data are presented in R/ϕ diagrams (Fig. 6); (2) the degree of shape preferred orientation expressed as a vector magnitude (Mardia 1972, V%, Table 1). V% is calculated as the sum of unit vectors (with orientation ϕ) weighted by R of each grain and tested for preferred orientation according to the Reyleigh test of Curray (1956). A distribution is not accepted as significantly different from random unless the probability, P, defined by Curray (1956, p. 125) is less than 0.05 (cf. Hara 1971); (3) the orientation of the resultant vector **R** (Mardia 1972, p. 20). This is compared with the orientation of S_L, S_{SH} and L_{SH} for each face (Table 1); (4) the grain size, expressed as the diameter of a circle with the same area as the ellipse used for approximation of the grain shape. The median grain size is given for each face (d, Table 1).

Samples from outside the Canisp Shear Zone (Group I, Table 1) show little or no shape fabric and no apparent relationship between the layering and the orientation of the resultant vector, **R**. All samples from Group II show a moderate to good shape fabric parallel to S_{SH}, and the samples from the transition zones (1 and 157) also have a shape fabric parallel to the intersection lineation between S_L and S_{SH}. Quartz has a strong shape fabric in the shear zone (Group III, Table 1), this is most pro-

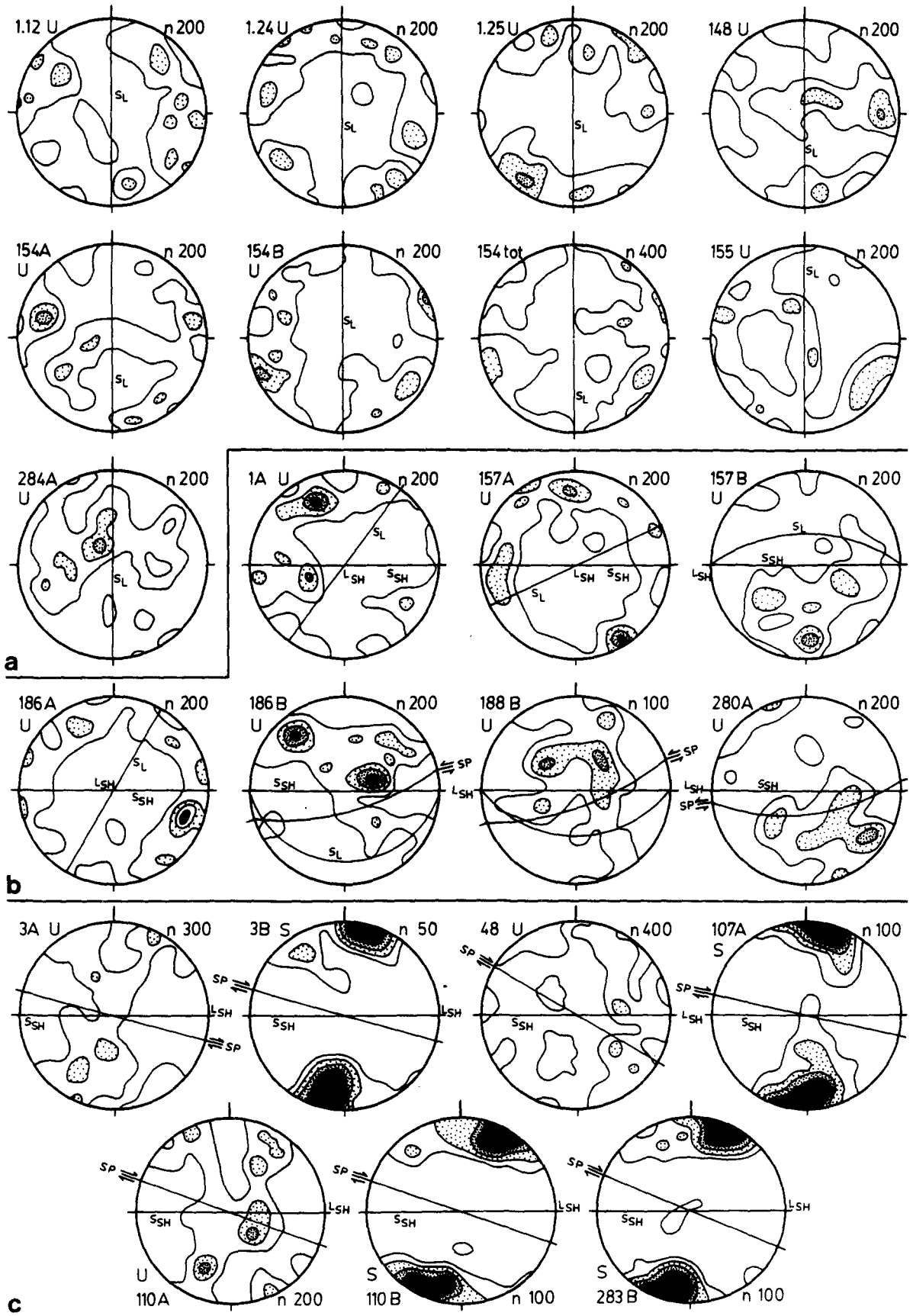

Fig. 7. Lower hemisphere equal-area plots of quartz *c*-axes. (a) Group I, (b) Group II, (c) Group III. n = number of measurements. S_L, S_{SH}, L_{SH} and SP: orientation of mesoscopic structures and the shear plane (with shear sense). Contoured at 1, 2, 3, ≥4 points per $100/n$% area. S = selective and U = unselective measurements. A and B indicate in which face the *c*-axes were measured (Table 1 gives orientation of these faces) but for convenience the fabric diagrams are presented with S_L vertical N–S and S_{SH} vertical E–W.

nounced in the faces parallel to L_{SH}. All samples affected by the shear episode show good agreement between the orientation of S_{SH} and the resultant vector. This makes it reasonable to assume that S_{SH} is the XY plane and L_{SH} the X direction of the finite strain ellipsoid.

Quartz fabric

The orientation of quartz *c*-axes has been analysed in 17 samples. Their locations are shown in Fig. 2, and in Table 1 their structural grouping and their modal quartz contents are listed. Faces were cut perpendicular to the foliation as previously described, and the *c*-axis orientations of 50, 100, 200, 300 or 400 grains were measured in each face (n, Table 1). The measurements are either selective, using only grains with banded extinction, or unselective, using all grains met in traverses perpendicular to the foliation (marked S or U in Table 1 and Fig. 7). The method of Starkey (1977) has been used for plotting, contouring, rotation and statistical analysis of the data. The parameters of the orientation patterns given in Table 1 are: (1) percentage of the area of the projection covered by 0 point concentration (equals empty space, E.S. %, Table 1); (2) maximum point concentration of the contoured diagram, expressed as points per 100/n% area (max., Table 1); (3) the data set is divided into 10 'sub-data sets' of equal size (n/10) and M0% (Table 1) express the mean empty space % of these with SD0% (Table 1) as standard deviation and (4) to evaluate whether a data set deviates significantly from a random distribution, i.e. the grains have a lattice preferred orientation, the method of Allison *et al.* (1978) is used. No fabric is regarded as significant unless $(M0\% - 36.8\%)/SD0\% \geq 2$. 36.8% is the empty space % of a random distribution (Starkey 1977).

The fabric diagrams from the layered gneisses (Fig. 7a) show rather low concentrations, and only two have a significant preferred orientation. No reproducible fabric pattern or any symmetry relations to S_L are found, i.e. the fabric is random and has spherical symmetry (Paterson & Weiss 1961). The samples from Group II (Fig. 7b) have a moderate fabric, only two are not significant. A weak but reproducible pattern consists of a pole-free area around the intersection lineation, with the axes concentrated in an irregular girdle perpendicular to this. The girdle may contain maxima at 0–30° and/or 60–90° from S_{SH} (Fig. 7b).

The sheared gneisses all have a moderate to strong preferred orientation of quartz (Table 1) and two types of reproducible fabric patterns (Fig. 7c). Unselective measurements give (with the exception of sample 48) a weak, asymmetric cross-girdle, with the girdles at 20–25° to Z, crossing at Y and with the best developed girdle perpendicular to the shear plane (3A and 110A, Fig. 7c). Selective measurements of grains with banded extinction give a strong point maximum perpendicular to the shear plane (3B, 107A, 110B, 283B, Fig. 7c). Both patterns have a monoclinic symmetry consistent with the shear sense of the shear zone.

DISCUSSION AND CONCLUSIONS

The physical constraints on the shear episode can be summarized as follows. Before the shear episode the gneisses in the shear zone were probably similar to those now found outside the shear zone. The stable paragenesis in both layered and sheared gneisses is plag–qz–hbl–bio–ep, and according to Sills (1982) the temperature was in the range 550–650°C or less during the Laxfordian shearing in the Lochinver area. The post-tectonic growth of hornblende in the sheared gneisses (Fig. 4f) indicates that amphibolite facies temperatures outlasted the shear episode. Syn-tectonic recrystallization caused a reduction in grain size of quartz and plagioclase, but the effect of the post-tectonic amphibolite facies temperatures on these minerals is uncertain. The equilibrium microstructure of plagioclase and quartz in the sheared gneisses (Figs. 4b & d) is the only evidence of post-tectonic grain growth of these minerals, and their present grain size is probably the same as when the shearing ended.

The microfabric shows that the shear episode generated a preferred orientation of quartz, and this is assumed to be the result of crystal plastic deformation. Undulose and banded extinction of quartz in the shear zone may be an evidence for crystal plastic behaviour, since White (1973) has shown, that such features result from recovery during and/or after deformation by dislocation creep and climb processes. Several recent workers (Bouchez 1977, Burg & Laurent 1978, Lister & Williams 1979) have shown that this deformation mechanism, with slip on one or more slip systems, can produce a shape and *c*-axis fabric in quartz, and the quartz microfabric of the Canisp Shear Zone is interpreted as a result of such processes.

Activation of different slip systems in quartz, and consequently the fabric pattern, depends on the temperature, stress, strain rate and possibly the water content (Tullis *et al.* 1973), while the symmetry of the fabric pattern reflects the symmetry of the deformation. The monoclinic symmetry of the fabric patterns from the Canisp Shear Zone is in agreement with the symmetry principles of Paterson & Weiss (1961) since the initial fabric has a spherical symmetry and simple shear a monoclinic symmetry. Such monoclinic fabric patterns, reflecting the kinematic framework of the deformation, are now well documented for shear zones (review: Lister & Williams 1979). According to Bouchez & Pecher (1981, fig. 14) the cross-girdles result from concurrent slip on basal $-$ a, prismatic $-$ $a \pm$ rhomb $-$ a slip systems, while the point maximum perpendicular to the shear plane reflects dominant slip on the basal $-$ a slip system.

Recent papers leave some doubt about the shear sense of the Canisp Shear Zone. Evans & Lambert (1974) assume that the shear direction is perpendicular to the linear structures in the shear zone, advocating a sinistral shear sense and an upward relative movement of the southern block (Fig. 8a). Based on the same assumptions Sheraton *et al.* (1973) proposed the opposite sense of

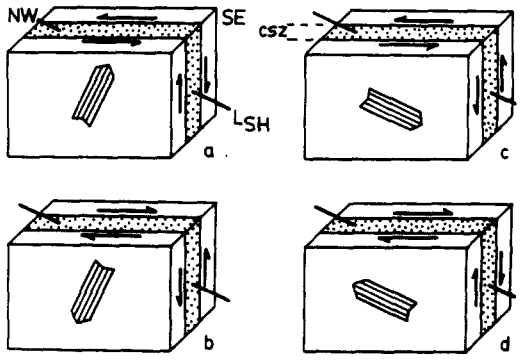

Fig. 8. Shear senses of the Canisp Shear Zone presented in recent papers: (a) Evans & Lambert (1974); (b) Sheraton *et al.* (1973); (c) Beach (1974); (d) Jensen (1980) and this paper.

movement (Fig. 8b). Beach (1974) used the Ramsay & Graham (1970) model for shear zones, with the shear direction subparallel to L_{SH}, and proposed a sinistral shear sense with downthrow of the southern block (Fig. 8c). The evidence presented here suggests a dextral shear sense subparallel to L_{SH} (Fig. 8d).

Acknowledgements—This work was carried out at the Department of Geology, Aarhus University, and supported by grants from the Danish Natural Science Research Council (grants No. 511-6712 and 511-8081 to Niels Ø. Olesen and Kai Sørensen). Thanks are given to colleagues at Aarhus University and University of Western Ontario for discussion and reading the manuscript. The paper has also benefited from constructive criticisms by the two anonymous reviewers.

REFERENCES

Allison, I., Kerrich, R. & Starkey, J. 1978. The variation of quartz orientation patterns in regional metamorphic tectonites. *Neues Jb. Miner. Abh.* **134**, 92–103.

Beach, A. 1974. The measurement and significance of displacements on Laxfordian shear zones, North West Scotland. *Proc. Geol. Ass.* **85**, 13–21.

Bouchez, J.-L. 1977. Plastic deformation of quartzites at low temperature in an area of natural strain gradient. *Tectonophysics* **39**, 25–50.

Bouchez, J.-L. & Pecher, A. 1981. The Himalayan main central thrust pile and its quartz-rich tectonites in central Nepal. *Tectonophysics* **78**, 23–50.

Brown, W. L., Macaudiere, J., Ohnenstetter, D. & Ohnenstetter, M. 1980. Ductile shear zones in a meta-anorthosite from Harris, Scotland: textural and compositional changes in plagioclase. *J. Struct. Geol.* **2**, 281–287.

Burg, J. P. & Laurent, Ph. 1978. Strain analysis of a shear zone in a granodiorite. *Tectonophysics* **47**, 15–42.

Curray, J. R. 1956. The analysis of two-dimensional orientation data. *J. Geol.* **64**, 117–131.

Etheridge, M. A. & Wilkie, J. C. 1979. The geometry and microstructures of a range of QP-mylonite zones—A field test of the recrystallized grainsize paleopiezometer. Proc. Conf. VIII, Analysis of actual fault zones in bedrock, *U.S. Geol. Surv. Open File Rep.* 79-1239, 448–504.

Evans, C. R. & Lambert, R. St-J. 1974. The Lewisian of Lochinver, Sutherland; the type area for the Inverian Metamorphism. *J. geol. Soc. Lond.* **130**, 125–150.

Flinn, D. 1962. On folding during three-dimensional progressive deformation. *Q. Jl geol. Soc. Lond.* **118**, 385–433.

Hara, I. 1971. An ultimate steady-state pattern of C-axis fabric of quartz in metamorphic tectonites. *Geol. Rdsch.* **60**, 1142–1173.

Jensen, L. N. 1980. Grundfjeldsgeologien af de Lewisiske gnejser i Lochinver området, NV Skotland. En strukturel, mikrostrukturel og kvarts-fabric undersøgelse. Unpublished thesis, Aarhus University.

Lister, G. S. & Williams, P. F. 1979. Fabric development in shear zones: theoretical controls and observed phenomena. *J. Struct. Geol.* **1**, 283–298.

Mardia, K. V. 1972. *Statistics of Orientational Data.* Academic Press, London.

Park, R. G. 1970. Observations on Lewisian Chronology. *Scott. J. Geol.* **6**, 379–399.

Paterson, M. S. & Weiss, L. E. 1961. Symmetry concepts in the structural analysis of deformed rocks. *Bull. geol. Soc. Am.* **72**, 841–882.

Ramsay, J. G. & Graham, R. H. 1970. Strain variation in shear belts. *Can. J. Earth Sci.* **7**, 786–813.

Sheraton, J. W., Tarney, J., Wheatley, T. J. & Wright, A. E. 1973. The structural history of the Assynt district. In: *The Early Precambrian of Scotland and Related Rocks of Greenland* (edited by Park, R. G. & Tarney, J.). University of Keele, Staffordshire, 31–44.

Sills, J. D. 1982. The retrogression of ultramafic granulites from the Scourian of NW Scotland. *Min. Mag.* **46**, 51–61.

Spry, A. 1969. *Metamorphic Textures.* Pergamon International Library, Oxford.

Starkey, J. 1977. The contouring of orientation data represented in spherical projection. *Can. J. Earth Sci.* **14**, 268–277.

Tullis, J., Christie, J. M. & Griggs, D. T. 1973. Microstructures and preferred orientations of experimentally deformed quartzites. *Bull. geol. Soc. Am.* **84**, 297–314.

White, S. 1973. The dislocation structures responsible for the optical effects in some naturally-deformed quartzes. *J. Mater. Sci.* **8**, 490–499.